

Banner appropriate to article type will appear here in typeset article

# Guidelines for authors

Alan N. Jones<sup>1†</sup>, H.-C. Smith<sup>1</sup> and J.Q. Long<sup>2</sup>

<sup>1</sup>STM Journals, Cambridge University Press, The Printing House, Shaftesbury Road, Cambridge CB2 8BS, UK

<sup>2</sup>DAMTP, Centre for Mathematical Sciences, Wilberforce Road, Cambridge CB3 0WA, UK

(Received xx; revised xx; accepted xx)

This file contains instructions for authors planning to submit a paper to the *Journal of Fluid Mechanics*. These instructions were generated in L<sup>A</sup>T<sub>E</sub>X using the JFM class file, and the source files for these instructions can be used as a template for submissions. The present paragraph appears in the abstract environment. All papers should feature a single-paragraph abstract of no more than 250 words, which provides a summary of the main aims and results. In addition to the figures in the main article a graphical abstract is now required. It will be used as a small thumbnail in the table of contents and on the abstract page, so multiple panels are not suitable and will be rejected. Please confirm that you have included an image to accompany your abstract, which will be used as the graphical abstract for manuscripts published in 2020. The image must be of aspect ratio 1.2:1 (e.g. 6cm x 5cm) and should be submitted in GIF or high resolution JPEG format (300 dpi). Unless very large, vector graphics are preferred to ensure image sharpness regardless of sizing. If you do not have the copyright to the image, please ensure you have permission to reuse the figure. Captions are not required. Text is actively discouraged, but if it must be used, it should be legible in a small thumbnail (2.4cmx2cm) presented in the table of contents. All graphical abstract images will be considered for a JFM cover selection by the JFM Panel. Please note that we publish 24 covers in a year.

**Key words:** Authors should not enter keywords on the manuscript, as these must be chosen by the author during the online submission process and will then be added during the typesetting process (see [Keyword PDF](#) for the full list). Other classifications will be added at the same time.

---

**MSC Codes** (*Optional*) Please enter your MSC Codes here

## 1. Introduction

Authors must submit using the online submission and peer review system [Scholar One](#) (formerly Manuscript Central). If visiting the site for the first time, users must create a new account by clicking on ‘register here’. Once logged in, authors should click on the

† Email address for correspondence: JFMEditorial@cambridge.org

‘Corresponding Author Centre’, from which point a new manuscript can be submitted, with step-by-step instructions provided. Authors must at this stage specify whether the submission is a *JFM Paper*, or a *JFM Rapids* paper (see §4 for more details). In addition, authors must specify an editor to whom the paper will be submitted from the drop-down list provided. Note that all editors exclusively deal with either *JFM Paper* or *JFM Rapids* (clearly indicated on the list), so please ensure that you choose an editor accordingly. Corresponding authors must provide a valid ORCID ID in order to submit a manuscript, either by linking an existing ORCID profile to your ScholarOne account or by creating a new ORCID profile. Once your submission is completed you will receive an email confirmation. Book reviews should not be submitted via the online submission site, but should instead be submitted by email to [anne.juel@manchester.ac.uk](mailto:anne.juel@manchester.ac.uk).

## 2. Methods

### 2.1. Particle Transport

#### 2.1.1. Translation and Rotation

Three coordinate frames are generally used to describe the position and orientation of ellipsoidal particles, which can be referred to as the inertial frame  $\mathbf{x}^{(in)} = [x^{(in)}, y^{(in)}, z^{(in)}]^T$ , the co-moving frame  $\mathbf{x}^{(cm)} = [x^{(cm)}, y^{(cm)}, z^{(cm)}]^T$  and the particle frame  $\mathbf{x}^{(p)} = [x^{(p)}, y^{(p)}, z^{(p)}]^T$ . The co-moving frame translates with the particle with its origin fixed at the particle centroid. The axes of the particle frame always coincide with the semi-axes of the ellipsoid. Thus, the particle frame also record particle rotation.

A point  $\mathbf{x}^{(in)}$  in the inertial frame can be transformed to the co-moving frame by

$$\mathbf{x}^{(cm)} = \mathcal{T} \mathbf{x}^{(in)} \quad (2.1)$$

Here, the translation matrix  $\mathcal{T}$  is defined as

$$\mathcal{T} = \begin{bmatrix} 1 & 0 & 0 & -x_p \\ 0 & 1 & 0 & -y_p \\ 0 & 0 & 1 & -z_p \\ 0 & 0 & 0 & 1 \end{bmatrix}, \quad (2.2)$$

with  $(x_p, y_p, z_p)$  being the coordinates of the particle centroid in the inertial frame. Transformation between the co-moving frame and the particle can be given as

$$\mathbf{x}^{(cm)} = \mathcal{R} \mathbf{x}^{(in)}. \quad (2.3)$$

The rotation matrix  $\mathcal{R}$  can be expressed by Euler angles  $(\phi, \theta, \psi)$  or quaternions  $(\varepsilon_1, \varepsilon_2, \varepsilon_3, \eta)$ . In this study, we follow Chesnutt & Marshall (2009) and write  $\mathcal{R}$  in the form of quaternions

$$\mathcal{R} = \begin{bmatrix} 1 - 2(\varepsilon_2^2 + \varepsilon_3^2) & 2(\varepsilon_1\varepsilon_2 + \varepsilon_3\eta) & 2(\varepsilon_1\varepsilon_3 - \varepsilon_2\eta) \\ 2(\varepsilon_2\varepsilon_1 - \varepsilon_3\eta) & 1 - 2(\varepsilon_3^2 + \varepsilon_1^2) & 2(\varepsilon_2\varepsilon_3 + \varepsilon_1\eta) \\ 2(\varepsilon_3\varepsilon_1 + \varepsilon_2\eta) & 2(\varepsilon_3\varepsilon_2 - \varepsilon_1\eta) & 1 - 2(\varepsilon_1^2 + \varepsilon_2^2) \end{bmatrix}. \quad (2.4)$$

The initial values of quaternions are determined by

$$\varepsilon_1 = \cos \frac{\phi - \psi}{2} \sin \frac{\theta}{2}, \quad \varepsilon_2 = \sin \frac{\phi - \psi}{2} \sin \frac{\theta}{2}, \quad \varepsilon_3 = \sin \frac{\phi + \psi}{2} \cos \frac{\theta}{2}, \quad \eta = \cos \frac{\phi + \psi}{2} \cos \frac{\theta}{2}. \quad (2.5)$$

65 Then quaternions are evolved by the following equation

$$66 \quad \begin{bmatrix} d\varepsilon_1/dt \\ d\varepsilon_2/dt \\ d\varepsilon_3/dt \\ d\eta/dt \end{bmatrix} = \frac{1}{2} \begin{bmatrix} \eta\Omega_x^{(p)} - \varepsilon_3\Omega_y^{(p)} + \varepsilon_2\Omega_z^{(p)} \\ \varepsilon_3\Omega_x^{(p)} + \eta\Omega_y^{(p)} - \varepsilon_1\Omega_z^{(p)} \\ -\varepsilon_2\Omega_x^{(p)} + \varepsilon_1\Omega_y^{(p)} + \eta\Omega_z^{(p)} \\ -\varepsilon_1\Omega_x^{(p)} - \varepsilon_2\Omega_y^{(p)} - \varepsilon_3\Omega_z^{(p)} \end{bmatrix}, \quad (2.6)$$

67 where  $\Omega_x^{(p)}$ ,  $\Omega_y^{(p)}$  and  $\Omega_z^{(p)}$  are the components of rotation rate in the particle frame.

68 The discrete element method (DEM) is employed to evolve particle movements. The  
69 governing equations of the linear and angular momentum are given as

$$70 \quad m \frac{d\mathbf{v}_i^{(in)}}{dt} = \mathbf{F}_{E,i}^{(in)} + \sum_{j \neq i} \mathbf{F}_{C,j \rightarrow i}^{(in)}, \quad (2.7)$$

$$71 \quad I_x^{(p)} \frac{d\Omega_{x,i}^{(p)}}{dt} - \Omega_{y,i}^{(p)} \Omega_{z,i}^{(p)} (I_y^{(p)} - I_z^{(p)}) = M_{E,i,x}^{(p)} + \sum_{j \neq i} M_{C,j \rightarrow i,x}^{(p)}, \quad (2.8)$$

$$72 \quad I_y^{(p)} \frac{d\Omega_{y,i}^{(p)}}{dt} - \Omega_{z,i}^{(p)} \Omega_{x,i}^{(p)} (I_z^{(p)} - I_x^{(p)}) = M_{E,i,y}^{(p)} + \sum_{j \neq i} M_{C,j \rightarrow i,y}^{(p)}, \quad (2.9)$$

$$73 \quad I_z^{(p)} \frac{d\Omega_{z,i}^{(p)}}{dt} - \Omega_{x,i}^{(p)} \Omega_{y,i}^{(p)} (I_x^{(p)} - I_y^{(p)}) = M_{E,i,z}^{(p)} + \sum_{j \neq i} M_{C,j \rightarrow i,z}^{(p)}. \quad (2.10)$$

74 Here,  $\mathbf{v}_i^{(in)}$  and  $\mathbf{\Omega}_i^{(p)} = [\Omega_{x,i}^{(p)}, \Omega_{y,i}^{(p)}, \Omega_{z,i}^{(p)}]^T$  are the velocity and rotation rate of particle  $i$ .  $m$  is  
75 the particle mass,  $\mathbf{I}^p = [I_x^{(p)}, I_y^{(p)}, I_z^{(p)}]^T$  is the moment of inertia with  $I_x^{(p)} = m(b^2 + c^2)/5$ ,  
76  $I_y^{(p)} = m(c^2 + a^2)/5$  and  $I_z^{(p)} = m(a^2 + b^2)/5$ .  $\mathbf{F}_{E,i}^{(in)}$  and  $\mathbf{M}_{E,i}^{(in)}$  are the electrostatic force and  
77 torque exerted on particle  $i$ .  $\mathbf{F}_{C,j \rightarrow i}^{(in)}$  and  $\mathbf{M}_{C,j \rightarrow i}^{(p)} = [M_{C,j \rightarrow i,x}^{(p)}, M_{C,j \rightarrow i,y}^{(p)}, M_{C,j \rightarrow i,z}^{(p)}]^T$  are  
78 the contact force and torque acting on particle  $i$  by particle  $j$ .

## 79 2.2. Collision between Ellipsoidal Particles

### 80 2.2.1. Collision Detection

81 In the particle frame of the  $i$ th particle, the ellipsoid can be written as

$$82 \quad \mathbf{X}^{(p)T} \mathbf{Q}_i^{(p)} \mathbf{X}^{(p)} = 0. \quad (2.11)$$

83 Here,  $\mathbf{X}^{(p)} = [x^{(p)}, y^{(p)}, z^{(p)}, 1]^T$  is the generalized position vector in the particle frame,  
84 and the characteristic matrix of ellipsoid  $i$  is

$$85 \quad \mathbf{Q}_i^{(p)} = \begin{bmatrix} 1/a^2 & 0 & 0 & 0 \\ 0 & 1/b^2 & 0 & 0 \\ 0 & 0 & 1/c^2 & 0 \\ 0 & 0 & 0 & -1 \end{bmatrix}. \quad (2.12)$$

86 For points in the inertial frame, the coordinates can be transformed to the particle frame  
87 through  $\mathbf{x}^{(p)} = \mathcal{RT} \mathbf{x}^{(in)}$ . Thus, the ellipsoid can be given in the inertial frame as

$$(\mathcal{RT}\mathbf{X}^{(in)})^T \mathbf{Q}_i^{(p)} (\mathcal{RT}\mathbf{X}^{(in)}) = \mathbf{X}^{(in)T} \mathcal{T}^T \mathcal{R}^T \mathbf{Q}_i^{(p)} \mathcal{RT} \mathbf{X}^{(in)} = \mathbf{X}^{(in)T} \mathbf{Q}_i^{(in)} \mathbf{X}^{(in)} = 0, \quad (2.13)$$

where  $\mathbf{Q}_i^{(in)} = \mathcal{T}^T \mathcal{R}^T \mathbf{Q}_i^{(p)} \mathcal{RT}$  is the  $4 \times 4$  characteristic matrix of ellipsoid  $i$  in the inertial frame.

If a point  $\mathbf{X}^{(in)}$  satisfies the equation of two different ellipsoids  $\mathbf{Q}_1^{(in)}$  and  $\mathbf{Q}_2^{(in)}$ , then two ellipsoids intersect at  $\mathbf{X}^{(in)}$ . Multiplying 2.13 of ellipsoid 1 by  $\lambda$  and subtracting 2.13 of ellipsoid 2 thus yields

$$\mathbf{X}^{(in)T} (\lambda \mathbf{Q}_1^{(in)} - \mathbf{Q}_2^{(in)}) \mathbf{X}^{(in)} = 0. \quad (2.14)$$

When two ellipsoids overlap, a family of non-trivial solutions  $\mathbf{X}^{(in)}$  exist to describe the intersection. Since  $\mathbf{Q}_1^{(in)}$  is invertible,  $\mathbf{Q}_1^{(in)-1} \mathbf{Q}_2^{(in)}$  should be singular. Thus, if two eigenvalues of  $\mathbf{Q}_1^{(in)-1} \mathbf{Q}_2^{(in)}$  are complex conjugates, two ellipsoid intersect (Alfano & Greer 2003).

### 2.2.2. Contact Point

When two ellipsoid intersect, the contact point is identified to calculate the contact interactions. In this study, the method of level surfaces are applied for contact point identification (Schneider & Eberly 2002; Ting 1992). (Note: cite paper on geometric potential algorithms by Ning (1992)) 2.13 can be expressed in the quadratic form as

$$P_i(\mathbf{x}^{(in)}) = \mathbf{x}^{(in)T} \mathcal{S}_i^{(in)} \mathbf{x}^{(in)} + \mathbf{b}_i^{(in)T} \mathbf{x}^{(in)} + c_i^{(in)} = 0. \quad (2.15)$$

Here,  $\mathcal{S}_i^{(in)}$ ,  $\mathbf{b}_i^{(in)}$  and  $c_i^{(in)}$  are defined by the components of  $\mathbf{Q}_i^{(in)}$

$$\mathcal{S}_i^{(in)} = \begin{bmatrix} q_{11}^{(in)} & q_{12}^{(in)} & q_{13}^{(in)} \\ q_{12}^{(in)} & q_{22}^{(in)} & q_{23}^{(in)} \\ q_{13}^{(in)} & q_{23}^{(in)} & q_{33}^{(in)} \end{bmatrix} \quad (2.16)$$

$$\mathbf{b}_i^{(in)} = 2[q_{14}^{(in)}, q_{24}^{(in)}, q_{34}^{(in)}]^T, \quad (2.17)$$

$$c_i^{(in)} = q_{44}^{(in)}. \quad (2.18)$$

The contact point on ellipsoid 1 is defined as the tangent point of ellipsoid 1 on the innermost level surface of ellipsoid 2. The level surfaces of ellipsoid 2 is given by

$$P_2(\mathbf{x}^{(in)}) = \alpha, \quad (2.19)$$

where  $\alpha < 0$  and  $\alpha > 0$  corresponds to the interior and exterior of ellipsoid 2. Then finding the contact point is equivalent to finding the minimum value of  $\alpha$  in 2.19 under the constraint of  $P_1(\mathbf{x}^{(in)}) = 0$ . By defining the Lagrangian function

$$\mathcal{L}(\mathbf{x}^{(in)}) = P_2(\mathbf{x}^{(in)}) + \tau P_1(\mathbf{x}^{(in)}) \quad (2.20)$$

for optimization, the contact point  $\mathbf{x}_{C,1}^{(in)}$  is given by

$$\mathbf{x}_{C,1}^{(in)} = -\frac{1}{2}(\mathcal{S}_2^{(in)} + \tau \mathcal{S}_1^{(in)})^{-1}(\mathbf{b}_2^{(in)} + \tau \mathbf{b}_1^{(in)}) = \frac{1}{\Phi(\tau)} \mathbf{y}(\tau), \quad (2.21)$$

where  $\Phi(\tau)$  is the determinant of  $(S_2^{(in)} + \tau S_1^{(in)})$ .  $\tau$  is the Lagrangian multiplier that can be obtained from the following six-order polynomial (see Chesnutt & Marshall 2009)

$$\mathbf{y}(\tau)^T S_1^{(in)} \mathbf{y}(\tau) + \Phi(\tau) \mathbf{b}_1^{(in)T} \mathbf{y}(\tau)^T + \Phi^2(\tau) c_1 = 0. \quad (2.22)$$

The above process can be repeated to identify the contact point of ellipsoid 2 on the level surfaces of ellipsoid 1.

### 2.2.3. Contact Forces and Torques

When two particles collide, the velocity at the contact point is

$$\mathbf{v}_{C,i}^{(in)} = \mathbf{v}_i^{(in)} + \boldsymbol{\Omega}_i^{(in)} \times \mathbf{r}_{C,i}^{(in)}, \quad (2.23)$$

where  $\mathbf{r}_{C,i}^{(in)} = \mathbf{x}_{C,i}^{(in)} - \mathbf{x}_{p,i}^{(in)}$  points from the ellipsoid centroid to the contact point. The normal velocity  $\mathbf{v}_{rel,n}^{(in)}$  and tangential velocity  $\mathbf{v}_{rel,t}^{(in)}$  are defined by

$$\mathbf{v}_{rel,n}^{(in)} = (\mathbf{v}_{C,i}^{(in)} - \mathbf{v}_{C,j}^{(in)}) \cdot \mathbf{n}, \quad (2.24)$$

and

$$\mathbf{v}_{rel,t}^{(in)} = (\mathbf{v}_{C,i}^{(in)} - \mathbf{v}_{C,j}^{(in)}) - (\mathbf{v}_{C,i}^{(in)} - \mathbf{v}_{C,j}^{(in)}) \cdot \mathbf{n}. \quad (2.25)$$

Here, the unit vector along the outward normal direction at the contact point are given by

$$\mathbf{n}(\mathbf{x}_{C,i}^{(in)}) = \nabla P_i(\mathbf{x}_{C,i}^{(in)}) / |\nabla P_i(\mathbf{x}_{C,i}^{(in)})|, \quad (2.26)$$

while the tangent unit vector equals

$$\mathbf{t} = \mathbf{v}_{rel,t}^{(in)} / |\mathbf{v}_{rel,t}^{(in)}|. \quad (2.27)$$

In each collision, particles are treated as soft spheres. The contact forces and torques are calculated according to the Hertz contact model (Marshall 2009).

$$\mathbf{F}_{C,j \rightarrow i}^{(in)} = (F_{ne} + F_{nd})\mathbf{n} + F_t \mathbf{t} \quad (2.28)$$

Here, the normal force consists of two terms, i.e., the normal elastic force  $F_{ne}$  and the normal damping force  $F_{nd}$ . The normal elastic force can be expressed as

$$F_{ne} = -k_N \delta_N. \quad (2.29)$$

$\delta_N = |\mathbf{x}_{C,i}^{(in)} - \mathbf{x}_{C,j}^{(in)}|$  is the normal overlap, and the stiffness  $k_N$  is written as

$$k_N = \frac{4}{3} E \sqrt{R \delta_N}, \quad (2.30)$$

The effective radius  $R$  is defined by the mean curvature of two ellipsoids at their contact points as

$$R = (K_{C,i} + K_{C,j})^{-1}, \quad (2.31)$$

with the local mean curvature  $K_i$  given by

$$K_i = \frac{h^3}{2} \left[ \frac{1}{a^2 b^2} \left( \frac{x_i^{(p)^2}}{a^2} + \frac{y_i^{(p)^2}}{b^2} \right) + \frac{1}{b^2 c^2} \left( \frac{y_i^{(p)^2}}{b^2} + \frac{z_i^{(p)^2}}{c^2} \right) + \frac{1}{c^2 a^2} \left( \frac{z_i^{(p)^2}}{c^2} + \frac{x_i^{(p)^2}}{a^2} \right) \right], \quad (2.32a)$$

$$h = [(x_i^{(p)})^2/a^4 + (y_i^{(p)})^2/b^4 + (z_i^{(p)})^2/c^4]^{-1/2}. \quad (2.32b)$$

The effective elastic modulus  $E$  is defined as

$$\frac{1}{E} = \frac{1 - \nu_i^2}{E_i} + \frac{1 - \nu_j^2}{E_j}, \quad (2.33)$$

where  $E_i$  and  $\nu_i$  are the elastic modulus and Poisson ratio of particle  $i$ . The normal damping force is proportional to the normal relative velocity

$$F_{nd} = -\eta_N \mathbf{v}_{rel} \cdot \mathbf{n}, \quad (2.34)$$

where the normal damping coefficient is defined as

$$\eta_N = \alpha_N (mk_N)^{1/2}. \quad (2.35)$$

Here,  $m$  is the particle mass, and  $\alpha_N$  is related to the coefficient of restitution  $e$  (Marshall 2009). The tangential force is calculated based on the static friction model and written as

$$F_t = -\mu_F |F_n| \quad (2.36)$$

where  $\mu_F = 0.3$  is the friction coefficient. Once the full contact force  $\mathbf{F}_{C,j \rightarrow i}^{(in)}$  is obtained, the corresponding rotation torque is computed by

$$\mathbf{M}_{C,j \rightarrow i}^{(in)} = \mathbf{r}_{C,ij}^{(in)} \times \mathbf{F}_{C,j \rightarrow i}^{(in)}. \quad (2.37)$$

### 2.3. Induced Charge

#### 2.3.1. Governing equation of surface charge

The electrostatic interactions between dielectrical ellipsoidal particles are considered using the techniques introduced by Barros *et al.* (2014); Barros & Luijten (2014). The governing equation of the induced charge (or the bound charge) on a dielectric surface is given by

$$\mathcal{A}\sigma_b = b \quad (2.38)$$

The left term of 2.38 is

$$\mathcal{A}\sigma_b = \bar{\kappa}\sigma_b + \varepsilon_0\Delta\kappa(\mathbf{E}_b + \mathbf{E}_{ext}) \cdot \mathbf{n}, \quad (2.39)$$

while the term on the right hand side writes

$$b = (1 - \bar{\kappa})\sigma_f - \varepsilon_0\Delta\kappa\mathbf{E}_f \cdot \mathbf{n}. \quad (2.40)$$

Here,  $\sigma_b$  and  $\sigma_f$  are the bound charge density and the free charge density, respectively.  $\bar{\kappa} = \kappa_p + \kappa_m$  is the mean dielectric constant of the particle ( $\kappa_p$ ) and the medium ( $\kappa_m$ ).  $\Delta\kappa = \kappa_p - \kappa_m$  is the difference of the dielectric constants.  $\varepsilon_0 = 8.854 \times 10^{-12} \text{ F/m}$  is the vacuum permittivity.  $\mathbf{E}_{ext}$  is the external field.  $\mathbf{E}_b$  is the electrical field induced by the bound charge at the particle surface, which reads

$$\mathbf{E}_b(\mathbf{r}_i) = \int_S \sigma_b(\mathbf{r}_j) \frac{\mathbf{r}_i - \mathbf{r}_j}{4\pi\varepsilon_0|\mathbf{r}_i - \mathbf{r}_j|^3} dS(\mathbf{r}_j). \quad (2.41)$$

$\mathbf{E}_f$  is the electric field induced by the free charge that can be obtained similar to 2.41.

### 2.3.2. Surface discretization

To implement 2.38, the ellipsoidal surface is discretized into uniform surface patches using the open-source code *DistMesh* developed by Persson & Strang (2004). Then the matrix in 2.38 can be written as

$$\mathcal{A}_{ij} = \bar{\kappa}_i \delta_{ij} + \Delta \kappa_i \mathbf{n}_i \cdot \mathcal{I}_{ij} \mathbf{a}_j \quad (2.42)$$

where the components of  $\mathcal{I}_{ij}$  is the Green function from the  $j$ th patch to the  $i$ th patch.

$$\mathcal{I}_{ij} = (\mathbf{r}_i - \mathbf{r}_j) / 4\pi |\mathbf{r}_i - \mathbf{r}_j|^3 \quad (2.43)$$

The Green function becomes singular when considering the contribution of each patch to itself ( $\mathcal{I}_{ii}$ ). In the present study, this contribution is omitted with

$$\mathcal{I}_{ii} = \mathbf{0}. \quad (2.44)$$

For approximations with higher-order accuracy, see Barros *et al.* (2014). Then the free charge  $\sigma_f$  is assumed to be uniformly distributed on the surface, and 2.38 is solved to get the bound charge density  $\sigma_b$ . The full charge density is then given as  $\sigma(\mathbf{r}_i) = \sigma_f(\mathbf{r}_i) + \sigma_b(\mathbf{r}_i)$ .

### 2.3.3. Electrostatic Force and Torque

The electrostatic force and torque can be directly computed by integrating the force and torque on each surface patch, which are shown as follows

$$\mathbf{F}_E = \int_S (\sigma_f + \sigma_b) \mathbf{E} dS, \quad \mathbf{M}_E = \int_S (\sigma_f + \sigma_b) \mathbf{r} \times \mathbf{E} dS. \quad (2.45)$$

## 3. Results and Discussions

For results and discussions.

## 4. Conclusion

For conclusion.

## Appendix A. Validation of the electrostatic interaction calculation

### A.1. Potential energy between a point charge and a dielectric sphere

The electrical potential energy  $U$  between a point charge  $q$  and a dielectric sphere with the radius of  $R$  and the dielectric constant  $\kappa_p$  is given by (J.D.Jackson 1999; Barros & Luijten 2014)

$$U = \frac{q^2}{8\pi\epsilon_0\kappa_m R} \sum_{n=0}^{\infty} \frac{(1 - \tilde{\kappa})n}{(1 + \tilde{\kappa})n + 1} \frac{1}{1 + (d/R)^{2(n+1)}}, \quad (\text{A } 1)$$

where  $\kappa_m$  is the dielectric constant of the medium,  $\tilde{\kappa} = \kappa_p / \kappa_m$  is the dielectric constant ratio,  $d$  is the distance from the point charge to the sphere surface. The electrical energy normalized by  $U_0 = q^2 / \epsilon_0 \kappa_m R$  shows good agreement with the theoretical solution in 1. Minor deviation occurs when  $d/R$  becomes small, which is due to the limited number of surface patches used here ( $N_{patch} = 956$ ). Increasing the total patch number or only refining the local surface patches could further increase the accuracy.

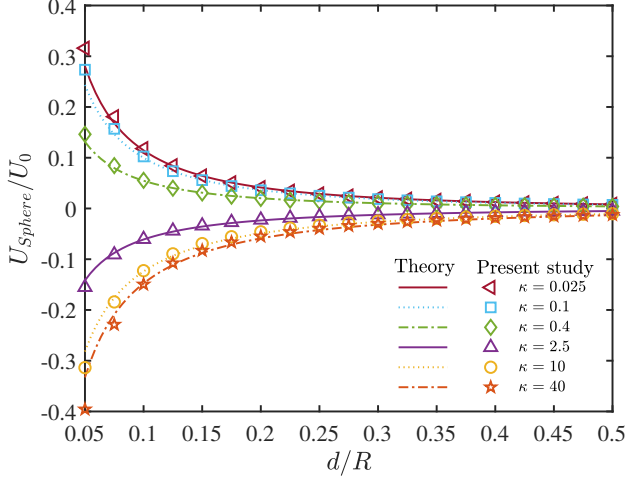


Figure 1: Normalized potential energy between a point charge and a dielectric sphere

### A.2. Electrostatic torque on ellipsoidal particle

For a neutral dielectric ellipsoidal particle defined by  $x^2/a^2 + y^2/b^2 + z^2/c^2 = 1$ , the electrostatic torque  $\mathbf{M}_E$  exerted by the external field  $\mathbf{E} = [E_x, E_y, E_z]$  is given by (T.B.Jones 1995)

$$M_{E,x} = \frac{4\pi\epsilon_m abc}{3} \cdot \frac{(\tilde{\kappa} - 1)^2 (L_z - L_y) E_z E_y}{[1 + (\tilde{\kappa} - 1)L_z][(\tilde{\kappa} - 1)L_y]}, \quad (\text{A } 2a)$$

$$M_{E,y} = \frac{4\pi\epsilon_m abc}{3} \cdot \frac{(\tilde{\kappa} - 1)^2 (L_x - L_z) E_x E_z}{[1 + (\tilde{\kappa} - 1)L_x][(\tilde{\kappa} - 1)L_z]}, \quad (\text{A } 2b)$$

$$M_{E,z} = \frac{4\pi\epsilon_m abc}{3} \cdot \frac{(\tilde{\kappa} - 1)^2 (L_y - L_x) E_y E_x}{[1 + (\tilde{\kappa} - 1)L_y][(\tilde{\kappa} - 1)L_x]}. \quad (\text{A } 2c)$$

Here, the elliptical integrals are defined as

$$L_x = \frac{abc}{2} \int_0^\infty \frac{ds}{(s + a^2)R_s}, \quad (\text{A } 3a)$$

$$L_y = \frac{abc}{2} \int_0^\infty \frac{ds}{(s + b^2)R_s}, \quad (\text{A } 3b)$$

$$L_z = \frac{abc}{2} \int_0^\infty \frac{ds}{(s + c^2)R_s}, \quad (\text{A } 3c)$$

with  $R_s = [(s + a^2)(s + b^2)(s + c^2)]^{1/2}$ . We consider a spheroid with  $b = c = 1$  and  $a$  ranging from 1 to 8 under an external field  $\mathbf{E} = E_0[1, 1, 1]$  (Add schematic). The dielectric constant of the particle and the medium is  $\kappa_p = 2.5$  and  $\kappa_m = 1$ . As shown in 2, the our calculation results coincide well with the theoretical solution in A 2.



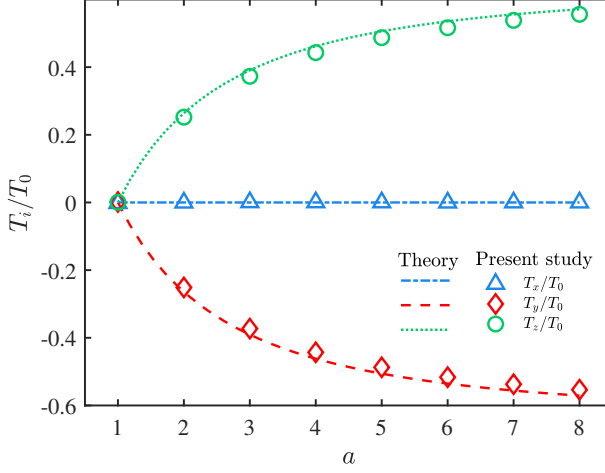


Figure 2: Normalized torque acting on the dielectric ellipsoid by the external field

---

$a$	1	2	3	4	5	6	7	8
$N_{patch}$	956	1564	2204	2812	3516	4092	4732	5340

---

Table 1: Number of patches  $N_{patch}$  of ellipsoids with a different semi-axis length  $a$ .

---

## Appendix B. Simulation acceleration using a reduced particle stiffness

In this appendix, the dimensionless linear momentum equation is derived in presence of the electrostatic interaction. And guidelines of adjusting the electrostatic force are given when a reduced elastic modulus is used for acceleration. When a charged particle encounters a head-on collision, the linear momentum equation (2.7) is

$$m \frac{d\mathbf{v}}{dt} = -(k_N \delta_N + \eta_N v_{rel,n}) \mathbf{n} + \mathbf{F}_E. \quad (\text{B } 1)$$

We introduce the dimensionless velocity  $\hat{\mathbf{v}}$  and the dimensionless overlap  $\hat{\delta}_N$  as

$$\hat{\mathbf{v}} = \mathbf{v}/v_0, \quad (\text{B } 2a)$$

$$\hat{\delta}_N = \delta_N/\delta_0. \quad (\text{B } 2b)$$

Here, the approaching velocity between two colliding particles is chosen as the characteristic velocity  $v_0$ , while the characteristic overlap is given by

$$\delta_0 = \left( \frac{mv_0^2}{ER^{1/2}} \right)^{2/5}. \quad (\text{B } 3)$$

Then B 1 becomes

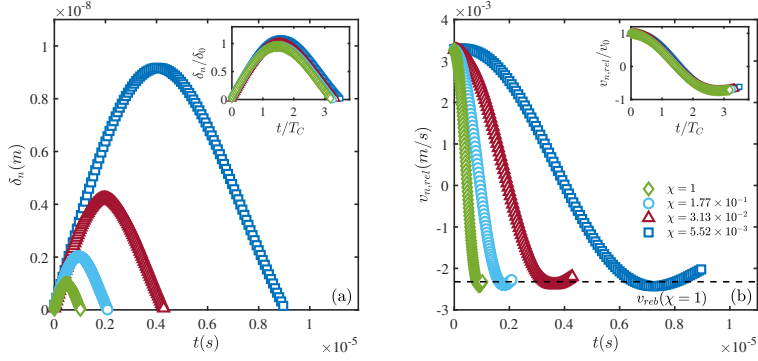


Figure 3: (a) Normal overlap and (b) normal relative velocity between two oppositely charged particles in a head-on collision with unmodified electrostatic force

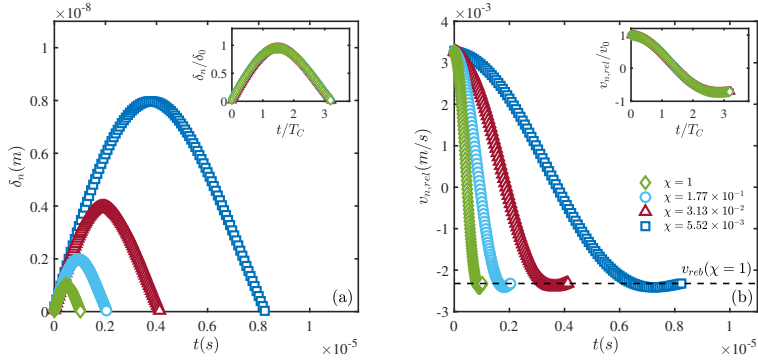


Figure 4: (a) Normal overlap and (b) normal relative velocity between two oppositely charged particles in a head-on collision with modified electrostatic force

$$\frac{d\hat{\mathbf{v}}}{d\hat{t}} + \frac{4}{3}\delta_N^{3/2}\mathbf{n} + \frac{2}{\sqrt{3}}\alpha_N\delta_N^{1/4}\hat{\mathbf{v}}_{rel,n}\mathbf{n} = \left(\frac{1}{m^3v_0^6E^2R}\right)^{1/5}\mathbf{F}_E. \quad (\text{B } 4)$$

After choosing a reduced elastic modulus  $E_R$ , the dimensionless electrostatic force

$$\hat{\mathbf{F}}_E = \left(\frac{1}{m^3v_0^6E^2R}\right)^{1/5}\mathbf{F}_E \quad (\text{B } 5)$$

should remain unchanged, so that B 4 gives the correct results. Thus, the dimensional electrostatic force should be modified as

$$\mathbf{F}_{E,R} = \left(\frac{E_R}{E_O}\right)^{2/5}\mathbf{F}_{E,O} = \chi^{2/5}\mathbf{F}_{E,O}. \quad (\text{B } 6)$$

Here, the subscripts  $O$  and  $R$  denote variables in a case with the original stiffness and that in a reduced case, respectively.  $\chi = E_R/E_O$  is the reduced ratio. (Add case discription here)

## REFERENCES

- 248 ALFANO, SALVATORE & GREER, MEREDITH L. 2003 Determining if two solid ellipsoids intersect. *Journal*  
 249 *of Guidance, Control, and Dynamics* **26** (1), 106–110.
- 250 BARROS, KIPTON & LUIJTEN, ERIK 2014 Dielectric effects in the self-assembly of binary colloidal aggregates.  
 251 *Phys. Rev. Lett.* **113**, 017801.
- 252 BARROS, KIPTON, SINKOVITS, DANIEL & LUIJTEN, ERIK 2014 Efficient and accurate simulation  
 253 of dynamic dielectric objects. *The Journal of Chemical Physics* **140** (6), 064903, arXiv:  
 254 <https://doi.org/10.1063/1.4863451>.
- 255 CHESNUTT, J.K.W. & MARSHALL, J.S. 2009 Blood cell transport and aggregation using discrete ellipsoidal  
 256 particles. *Computers and Fluids* **38**, 1782–1794.
- 257 J.D.JACKSON 1999 *Classical Electrodynamics*. Wiley.
- 258 MARSHALL, J.S. 2009 Discrete-element modeling of particulate aerosol flows. *Journal of Computational*  
 259 *Physics* **228** (5), 1541–1561.
- 260 PERSSON, P.-O. & STRANG, G. 2004 A simple mesh generator in matlab. *SIAM Review* **46**, 329–345.
- 261 SCHNEIDER, PHILIP & EBERLY, DAVID H 2002 *Geometric tools for computer graphics*. Elsevier.
- 262 T.B.JONES 1995 *Electromechanics of Particles*. Cambridge University Press.
- 263 TING, JOHN M 1992 A robust algorithm for ellipse-based discrete element modelling of granular materials.  
 264 *Computers and Geotechnics* **13** (3), 175–186.